

See discussions, stats, and author profiles for this publication at: <https://www.researchgate.net/publication/351274578>

Electrochemical oxidation of paracetamol on boron-doped diamond electrode: analytical performance and paracetamol degradation

Article · April 2021

DOI: 10.5599/jese

CITATIONS

10

READS

57

4 authors:



Kouakou Etienne Kouadio
University "Félix Houphouët-Boigny"

5 PUBLICATIONS 14 CITATIONS

[SEE PROFILE](#)



Kambire Ollo
Université de Man, Ivory Coast

32 PUBLICATIONS 131 CITATIONS

[SEE PROFILE](#)



Konan Sylvestre Koffi
University "Félix Houphouët-Boigny"

14 PUBLICATIONS 29 CITATIONS

[SEE PROFILE](#)



Ouattara Lassine
University "Félix Houphouët-Boigny"

54 PUBLICATIONS 933 CITATIONS

[SEE PROFILE](#)

Some of the authors of this publication are also working on these related projects:



Treatment of Hospital Wastewaters in Ivory Coast and Colombia by Advanced Oxidation Processes [View project](#)



Fonds National Suisse IZ01Z0_146919 [View project](#)



Original scientific paper

Electrochemical oxidation of paracetamol on boron-doped diamond electrode: analytical performance and paracetamol degradation

Kouakou E. Kouadio¹, Ollo Kambiré², Konan S. Koffi¹, Lassiné Ouattara¹✉

¹Laboratoire de constitution et réaction de la matière, UFR SSMT, Université Félix Houphouët-Boigny de Cocody, Abidjan, 22 BP 582 Abidjan 22, Côte d'Ivoire

²UFR Sciences et Technologies, Université de Man, BP 20 Man, Côte d'Ivoire

Corresponding author: ✉ ouatlassine@yahoo.fr

Received: November 16, 2020; Revised: February 6, 2021; Accepted: February 7, 2021

Abstract

Electrochemical oxidation of paracetamol on boron-doped diamond (BDD) anode has been studied by cyclic voltammetry and preparative electrolysis. Quantification of paracetamol during electrolysis has been mainly realized by differential pulse voltammetry technique in the Britton-Robinson buffer solutions used as the supporting electrolyte. Various parameters such as current intensity, nature of the supporting electrolyte, temperature, and initial concentration of paracetamol have been investigated. The electrochemical characterization by the outer sphere Fe(III)/Fe(II) redox couple has also been performed, showing the metallic character of BDD electrode. The obtained linear dependency of the oxidation peak current intensity and paracetamol concentration indicates that BDD electrode can be used as an electrochemical sensor for the detection and quantification of paracetamol. The investigation of paracetamol degradation during preparative electrolysis showed that: (i) the degradation rate of paracetamol increases with increase of current intensity applied; (ii) for the initial concentrations of 10, 6 and 1 mM of paracetamol, its oxidation rate reaches 60, 78 and 99 % respectively, after 1 h of electrolysis in 0.3 M H₂SO₄ (pH 0.6) at applied current density of 70 mA cm⁻²; (iii) at temperatures of electrolyte solution of 28, 55 and 75 °C, paracetamol oxidation rate reached 85, 92 and 97 % respectively, after 2 h at applied current density of 70 mA cm⁻². From the investigation of the effect of pH value of electrolyte solution, it appears that oxidation of paracetamol is more favorable in acidic solution at pH 3 than solutions of higher pH values.

Keywords

Boron-doped diamond; paracetamol; electrolysis; voltammetry; oxidation; degradation.

Introduction

Paracetamol, known also as acetaminophen, is one of the most commonly used analgesics (pain relievers) and antipyretics (anti-fever) for humans today [1-3]. It is present in Doliprane®, Efferalgan® or Di-antalvic®, which are the most sold drugs in pharmacies. Efficacy, good tolerance, pharmacokinetic profile, cost and acceptability make paracetamol to be the first-line drug for treatment of mild to moderate pains. Paracetamol is generally available in 500 mg tablets, and also in the soluble form (sachets, effervescent tablets), or liquid preparations for young children [2,4]. The intensive use of paracetamol leads to its presence in the environment, and more specifically in the surrounding waters. This makes a real problem for humans and other living things, since paracetamol breaks down into very toxic metabolites [5-8]. A general awareness is therefore necessary in order to propose effective methods for detection, quantification and decontaminating wastewaters containing paracetamol.

According to the literature [9-12], physical, biological and chemical methods are usually used in wastewaters treatment. Thus, activated carbon is widely used to treat organic and inorganic pollutants [13,14] and also, to immobilize metal ions such as copper, zinc, cadmium or chromium [15]. The main limitation of such treatment lies in the fact that in any case, pollutants are not degraded, but concentrated on the activated carbon which must be subsequently treated in order to regenerate it. Biological methods for wastewater treatment are based on the use of microorganisms under aerobic or anaerobic conditions [16]. Faced with toxic compounds that are difficult to biodegrade, however, these microorganisms proved to be rather inefficient.

Due to shortcomings of these treatment methods, over the past decade much research was focused on the new class of oxidation techniques, known as the advanced oxidation processes (POA). POA is designed to remove organic and inorganic materials in water and wastewater by the oxidation process. This technology has already shown its effectiveness in the treatment of toxic and biologically refractory organic pollutants. Along to all these treatments, the electrochemical treatment must also be considered. Compared to other conventional processes such as Fenton process for water and wastewater treatment and processes using ultraviolet radiation [17-19], the electrochemical treatment has three major advantages: high efficiency, rapid reaction, and easy implementation. In addition, electrochemical oxidation processes consume few chemicals and produce no waste.

According to the literature, the electrochemical method has shown its effectiveness in the treatment of wastewater containing organic pollutants [20-22]. The effectiveness of the electrochemical treatment depends strongly on the properties of electrode used as the anode in the case of electrolysis [10,23,24]. In this work, the boron-doped diamond (BDD) electrode is used. BDD has remarkable optical, electronic, and mechanical qualities, thus showing a great aptitude for various applications in different fields. According to literature, BDD can allow complete mineralization of organic compounds [21,24].

Electrochemical methods such as square wave voltammetry (SWV), cyclic voltammetry (CV) and differential pulse voltammetry (DPV) have already been used for the determination of concentrations of organic compounds [1,25-29]. Also, it was already shown that DPV provides good limit of detection for paracetamol using boron-doped diamond electrode [1,25]. In this study, the follow-up of paracetamol concentration during its oxidation will be performed by DPV technique, using BDD electrode as the sensor.

Experimental

Electrochemical measurements

The voltammetric measurements were performed using an Autolab PGSTAT 20 (Ecochemie) connected to a potentiostat equipped with USB electrochemical interface. This system is connected to a three-electrode single compartment glass cell and a computer for data storage and processing. GPES 4 software was employed to get voltammograms. The glass electrochemical cell consisted of saturated calomel electrode (SCE) and platinum wire as the reference and counter electrode, respectively. BDD electrode with a surface of 1 cm² was used as the working electrode. All pH values were measured with a pH meter. All potential values are reported against standard hydrogen electrode (SHE), calculated according to the following relation:

$$E_{\text{SHE}} = E_{\text{SCE}} + 0.25 \quad (1)$$

Electrodes

Boron doped diamond (BDD) electrodes were prepared by hot-filament chemical vapor deposition (HF-CVD) on low resistivity (1-3 mΩ cm) p-Si wafers (siltronix, diameter 10 cm, thickness 0.5 mm). The process gas was a mixture of 1 % CH₄ in H₂ containing trimethylboron. Film was grown at a rate of 0.24 μm h⁻¹. The film thickness was about 1 μm.

Chemicals

Paracetamol was purchased from a pharmacy in Abidjan. All chemicals used in the experiments were reagent grade or higher, and used as received without any further purification. Sulfuric acid (96 %), iron (II) sulfate (99 %) and sodium hydroxide (98 %) were obtained from PanReac Quimica Sau. Orthophosphoric acid (85 %) and boric acid (99.5 %) were obtained from Emsure® brand. Ammonium iron (III) sulfate (99 %) was obtained from Merck, while acetic acid (99.7 %) was obtained from Emparta®. The working solutions for voltammetric investigations were prepared by dilution of the stock solution. All solutions were protected from light and used within 24 h to avoid decomposition. Distilled water was used to prepare supporting electrolytes.

Britton-Robinson buffer solution preparation

Britton-Robinson buffer solution, 0.04 M, was prepared in order to maintain pH value of the samples taken during the electrolysis within a very restricted range. For this purpose, acetic acid, orthophosphoric acid and boric acid were used in the respective amounts of 4.6 mL, 5.4 mL, and 4.9713 g per 2 L of solution [30].

The preparation of this buffer solution was done as follows: a certain amount of water in a glass beaker was heated to a temperature of around 70 °C using a water bath. Then, boric acid was added into heated water and left to cool. The cooled solution of boric acid was transferred into 2000 mL flask containing above-mentioned quantities of acetic acid and orthophosphoric acid, filled with distilled water to mark and homogenized. In 99 mL of this Britton-Robinson buffer solution, 1 mL of paracetamol samples taken from electrolysis at pre-established time intervals were added. After homogenization of solution, differential pulse voltammograms (DPVs) were recorded using electrochemically pretreated BDD electrode, in order to determine paracetamol concentrations.

Preparative electrolysis

For preparative electrolysis, BDD was used as the anode and zirconium plate as the cathode. These two electrodes of 16 cm² each were separated by 2 cm, what delimited the cell-volume to 32 cm³. The solution was recirculated using a mini peristaltic pump of the Watson Marlow 505U

type. The flow rate of the solution was 2.7 mL s^{-1} . Fabrimex 141 type voltage generator allowed to keep the current constant during the electrolysis. Batch mode setup was used for electrolysis.

Setup for analytical measurements

Prior to the application of differential pulse voltammetry, BDD electrode was electrochemically pretreated. Cyclic voltammetry was applied by seven cycles aiming to purify BDD in 0.5 M sulfuric acid with previously cathodically pretreated BDD electrode at -2 V during 90 s [31]. Well cleaned electrode was immersed in the Britton-Robinson buffer solution without paracetamol and anodically pretreated at 2 V for 15 s. Finally, the pretreated BDD electrode was used to analyze the content of paracetamol using DPV technique in different supporting electrolytes after homogenization *via* a magnetic bar coupled to a magnetic stirrer. DPV curves were obtained under the following conditions: $E_p = -2 \text{ V}$; $t_p = 90 \text{ s}$; modulation time $\geq 0.05 \text{ s}$; potential scan rate = 70 mV s^{-1} .

For the determination of limits of detection (LOD) and quantification (LOQ) of paracetamol, the following equations were used:

$$\text{LOD} = 3 S_D / b \quad (2)$$

$$\text{LOQ} = 10 S_D / b \quad (3)$$

where S_D is the standard deviation of blank current signals and b is the slope of the calibration curve [26].

Results and discussion

Electrochemical characterization of BDD electrode

In order to investigate the electrochemical behavior of the prepared BDD electrode, Fe(III)/Fe(II) redox couple was used, and the influence of its concentration (20-50 mM) on the electrode response was studied in 0.3 M sulfuric acid solution as the supporting electrolyte. The obtained results are presented in Figure 1(a), showing oxidation peak in the forward potential scan and reduction peak in the backward potential scan. The anodic and cathodic peaks correspond to the oxidation and reduction of the redox couple considered. The peaks observed are typical for electrodes that are good electronic conductors [24,31,32].

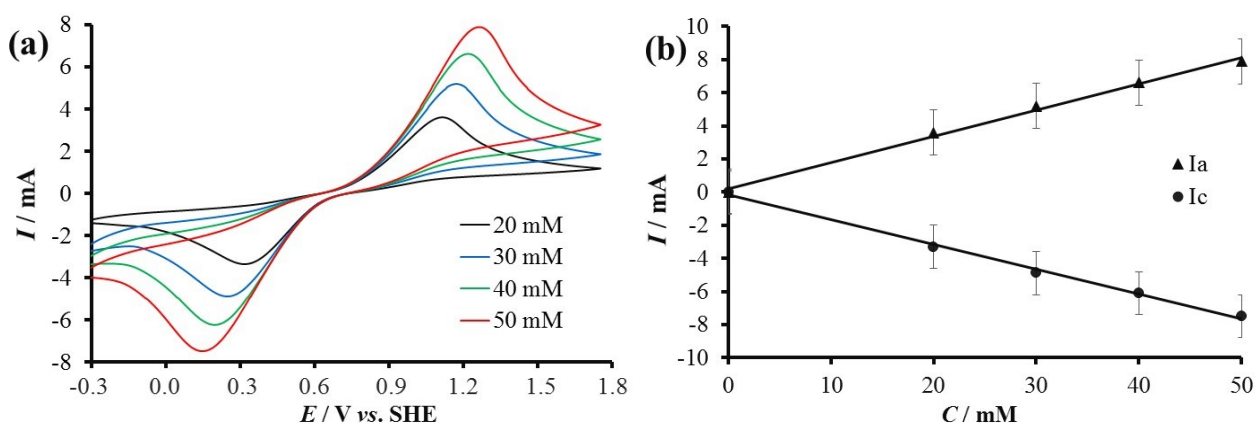


Figure 1. (a) Cyclic voltammetry (50 mV/s) of BDD electrode at different concentrations of Fe(III)/Fe(II) redox couple in 0.3 M H₂SO₄; (b) anodic and cathodic peak current intensity against Fe(III)/Fe(II) concentration; T = 25 °C

Figure 1(a) also shows that the current intensities of the anodic and cathodic peak increase in absolute values with increase of the concentration of redox species. Anodic and cathodic peak current intensities plotted as a function of redox species concentration, led to straight lines passing

through the origin of the axes (Figure 1(b)). These results show that oxidation and reduction reactions of redox species are responsible for the appearance of these peaks. The results are similar to that obtained with good electronic conductor electrodes such as metallic electrodes. Thus, the metallic character of the used BDD electrode is generally approved [24,31]. The proportionality observed between the current intensity and concentration of the redox couple studied suggests that BDD electrode can principally be used as an electrochemical sensor for detection and quantification of paracetamol, and possibly other pharmaceutical organics in aqueous solutions [1,31].

Cyclic voltammetry investigations were carried out at several potential scan rates for an equimolar concentration (50 mM) of the redox couple Fe(III)/Fe(II). Figure 2(a) shows the obtained cyclic voltammograms. In this figure, the current intensities of the anode and cathode peak increase in absolute values with increase of potential scan rates. In Figure 2(b), the anodic and cathodic peak current intensities have been represented as a function of the square root of the potential scan rate. It appears that the peak current intensities are proportional to the square root of the potential scan rates, since straight lines passing through the origin of the axes were obtained. This confirms the quasi-reversible nature of Fe(III)/Fe(II) redox reaction on BDD, what has already been observed previously in our laboratory [24,31]. The linearity between the peak current intensity and the square root of the potential scan rates indicates that the oxidation-reduction kinetics at the electrode is diffusion-controlled [24].

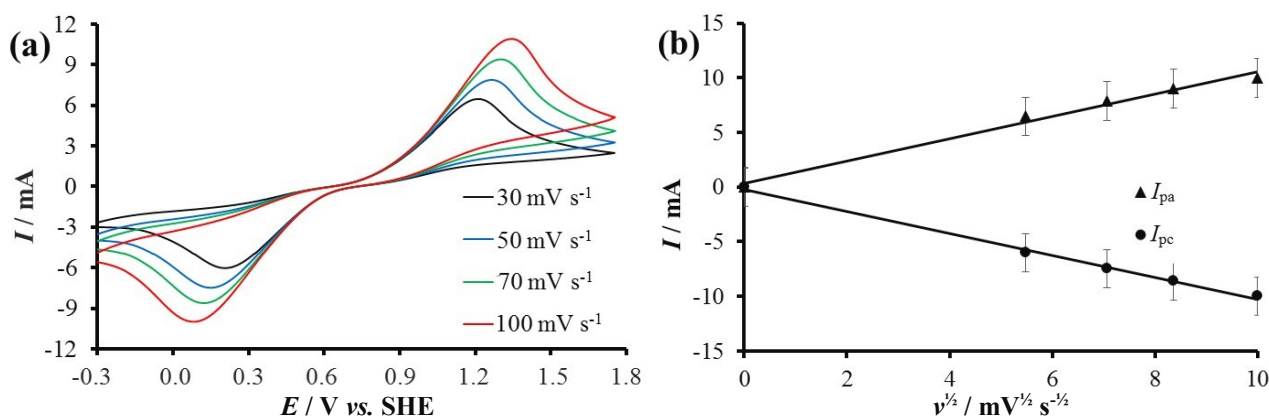


Figure 2. (a) Cyclic voltammetry of Fe(III)/Fe(II) redox couple (50 mM) in 0.3 M H₂SO₄ on BDD at different potential scan rates; (b) anodic and cathodic peak current intensities against square root of the scan rate; T = 25 °C

Cyclic voltammetry of paracetamol oxidation

The electrochemical behavior of BDD in 0.3 M sulfuric acid solution in the presence of several paracetamol concentrations at the potential scan rate of 100 mV s⁻¹ is presented in Figure 3(a). This figure shows increase in the current values around 0.9 V, followed by an irreversible oxidation peak at 1.05 V. This peak characterizes the anodic oxidation of paracetamol.

Figure 3(a) shows that as the paracetamol concentration increases, the current intensity of the oxidation peak also increases. This indicates the direct oxidation of paracetamol on BDD electrode. The plot of the oxidation peak current intensity against the concentration of paracetamol shown in Figure 3(b), led to the straight line passing through the origin of the axes. The slope of this straight line is about 0.4 mA mol⁻¹, with determination coefficient of 0.99. Hence, BDD electrode can be a good candidate for detection and quantification of paracetamol.

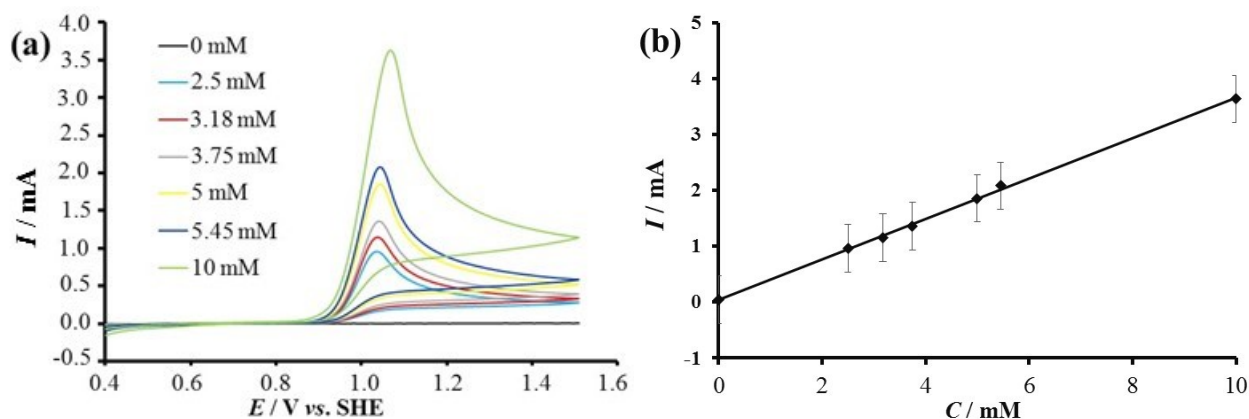


Figure 3. (a) Cyclic voltammograms (100 mV s^{-1}) of BDD electrode at different concentrations of paracetamol in $0.3 \text{ M H}_2\text{SO}_4$ solution; (b) anodic peak current intensity as a function of paracetamol concentration; $T = 25 \text{ }^\circ\text{C}$

Effect of the supporting medium

In order to determine the ideal supporting electrolyte for the quantification of paracetamol during electrolysis, calibration curves of paracetamol in sulfuric acid, orthophosphoric acid and Britton-Robinson buffer solutions were carried out.

Figure 4(a) represents DPV curves for paracetamol concentrations varying from 2 to 91 μM in 0.3 M sulfuric acid solution. It can be noticed in Figure 4(a) that the peak potential values of paracetamol oxidation are approximately equal, whereas the intensity of the oxidation peak current increases with the increase of paracetamol concentration. In Figure 4(b), the peak current intensity is plotted against the concentration of paracetamol, showing two linear regions. One linear region is characteristic for low concentrations of paracetamol below $10 \mu\text{M}$, and the other for concentrations of paracetamol higher than $10 \mu\text{M}$. In the insert of Figure 4(b), the straight line determined in the low concentration range of paracetamol is shown. Its equation was evaluated as: $I = 2.4698 C + 1.3764$ with determination coefficient of $R^2 = 0.972$. The limits of detection and quantification were determined using equations (2) and (3), and the obtained values $\text{LOD} = 0.37 \mu\text{M}$ and $\text{LOQ} = 1.23 \mu\text{M}$.

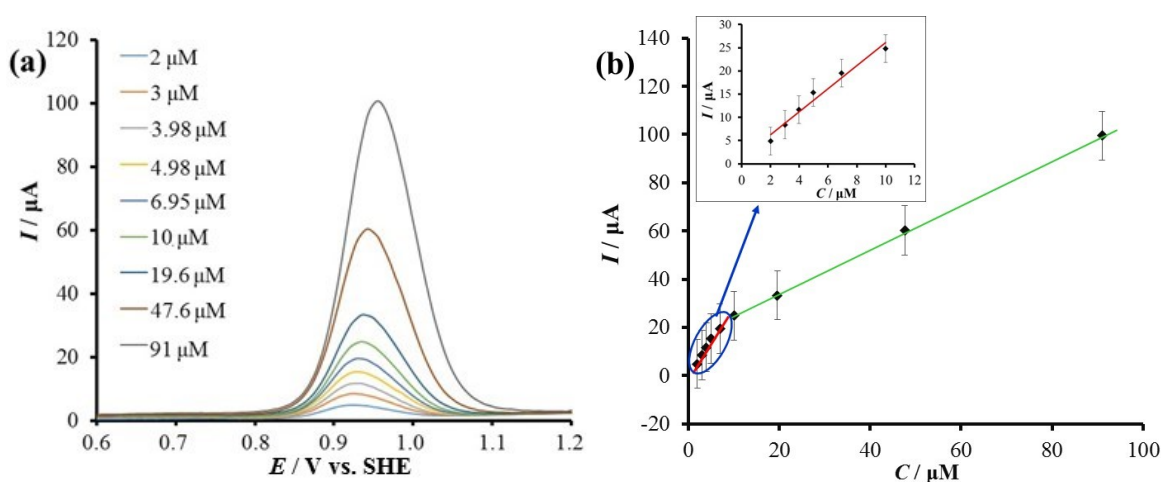


Figure 4. (a) Differential pulse voltammograms of BDD electrode for different concentrations of paracetamol in $0.3 \text{ M H}_2\text{SO}_4$; (b) current intensity calibration curve as a function of paracetamol concentration; $T = 25 \text{ }^\circ\text{C}$

Orthophosphoric acid (0.3 M) was also chosen as the supporting electrolyte containing several concentrations of paracetamol. The obtained DPV results are shown in Figure 5(a). Here also, the

current intensity of paracetamol oxidation peak increases with the increase of concentration of paracetamol. Figure 5(b) presents the peak current intensity as a function of paracetamol concentration. The obtained results are quite similar to these obtained in sulfuric acid. In orthophosphoric acid supporting electrolyte, two linear regions, one for low concentrations and the other for high concentrations of paracetamol, were also obtained. In the low paracetamol concentration range (insert of Figure 5(b)), the straight line is characterized by the following equation: $I = 1.9232 C + 4.6364$ with $R^2 = 0.997$. In orthophosphoric acid supporting electrolyte containing paracetamol, LOD and LOQ of paracetamol were estimated as 0.47 and 1.57 μM , respectively.

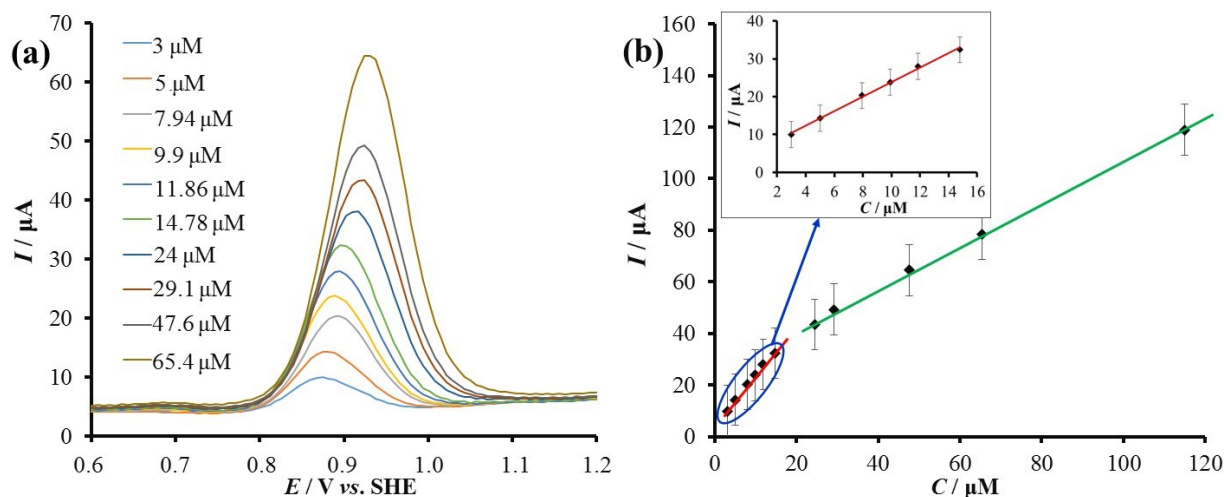


Figure 5. (a) Differential pulse voltammograms of BDD electrode for different concentrations of paracetamol in 0.3 M H_3PO_4 ; (b) current intensity calibration curve as a function of paracetamol concentration; $T = 25^\circ\text{C}$

Figure 6(a) highlights DPV curves obtained in 0.04 M Britton-Robinson buffer solution.

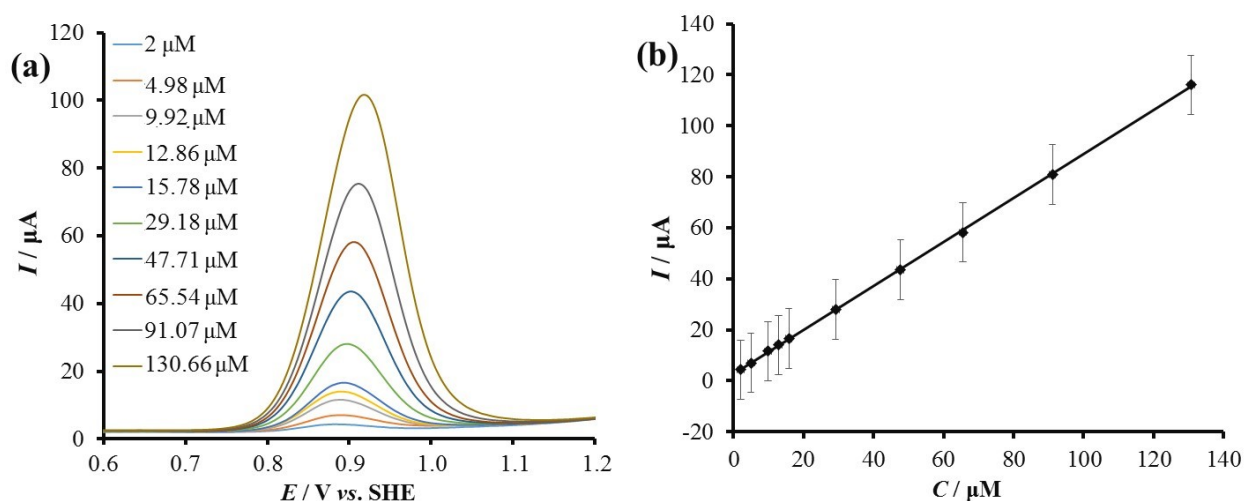


Figure 6. (a) Differential pulse voltammograms of BDD electrode for different concentrations of paracetamol in 0.04 M Britton-Robinson buffer solution; (b) current intensity calibration curve as a function of paracetamol concentration; $T = 25^\circ\text{C}$

Here also, the oxidation peak potential values associated with each concentration of paracetamol are equal, while the peak current intensity increases linearly with paracetamol concentration (Figure 6(b)). This straight line passes through the origin of the axes and its equation is evaluated as: $I = 0.8615 C + 2.7177$ with determination coefficient of 0.999. LOD and LOQ values for paracetamol in Britton-Robinson buffer solution were calculated as 0.167 and 0.559 μM , respectively.

From the results presented in Figures 4-6, it appears that the Britton-Robinson buffer solution leads to the best calibration curve, which explores the highest paracetamol concentration range (2.0-130.66 μM) and shows the lowest LOD and LOQ values (0.167 and 0.559 μM). As have already been shown for electroanalytical determinations of some other drugs [33,34], Britton-Robinson buffer solution is confirmed also in our experimental conditions as the most suitable solution for monitoring concentrations of paracetamol during its electrolysis.

Up to now, paracetamol was determined by various electrochemical methods using various electrode materials. A comparison of our findings with some literature data [31,35-44] is presented in Table 1.

Data in Table 1 clearly show that the detection limit of 0.167 μM determined in this work is in accordance or even better than other literature data, indicating that our determination method could be a reliable method for the determination not only of paracetamol, but also traces of some other organic pharmaceutical compounds present in wastewaters. In further experiments, this method will be used to follow the evolution of paracetamol concentration during its degradation.

Table 1. Efficiency of some modified electrodes in determination of paracetamol by various voltametric methods

Electrode	Method	Linear working range of paracetamol concentration, μM	Detection limit of paracetamol concentration, μM	Reference
PANI/MWCNT/GCE	SWV	1 - 100	0.25	[35]
C ₆₀ /GCE	DPV	50 - 1500	5	[36]
Nafion/TiO ₂ -graphene/GCE	DPV	1 - 100	0.21	[37]
AuNP-PGA/SWCNT	DPV	8.3 - 145.6	1.18	[38]
PAY/nano-TiO ₂ /GCE	DPV	12 - 120	2.0	[39]
MIP	DPV	1 - 4000	0.33	[40]
Nevirapine/CPE	DPV	20 - 250	0.77	[41]
GR-CS/GCE	DPV	1-100	0.3	[42]
CS/CPE	SWV	0.8 to 200	0.51	[43]
PMMCNTPE	CV	2.0-50	0.38	[44]
BDD	DPV	1.98 - 13.87	0.16	[31]
BDD	DPV	2.0-130.66	0.167	This work

GCE: glassy carbon electrode; CPE: carbon paste electrode; BDD: boron doped diamond electrode; DPV: differential pulse voltammetry; SWV: square-wave voltammetry; CV: cyclic voltammetry; PGA: poly (glutamic acid); PAY: poly (acid yellow 9); SWCNT: single-walled carbon nanotubes; PANI-MWCNT: polyaniline-multi-walled carbon nanotubes composite; MIP: molecular imprinted polymeric micelles; GR-CS: graphene-chitosan composite; CS: chitosan; PMMCNTPE: poly(methyl) orange modified carbon nanotube paste electrode.

Electrolysis of paracetamol

The effect of current density on paracetamol oxidation during electrolysis was also studied. For such a purpose and in order to determine the optimal current density, the electrolysis experiments were conducted in 0.3 M H₂SO₄ solution under current densities of 20, 50, 70 and 100 mA cm⁻². DPVs of paracetamol samples in Britton-Robinson buffer solution, subjected previously (10 mM) to electrolysis in 0.3 M H₂SO₄ at different current density values and taken after different electrolysis time, are shown in Figure 7. In this figure, differential pulse voltammograms show a decrease of oxidation current peak intensities of paracetamol with the electrolysis time. The decrease of the peak current intensity is rapid and highly marked as the applied current density increases. The oxidation peak current of paracetamol is observed at around 0.9 V. At higher electrolysis time, however, another current peak appears at 0.55 V. This new peak firstly increases in intensity and then decreases until it disappears.

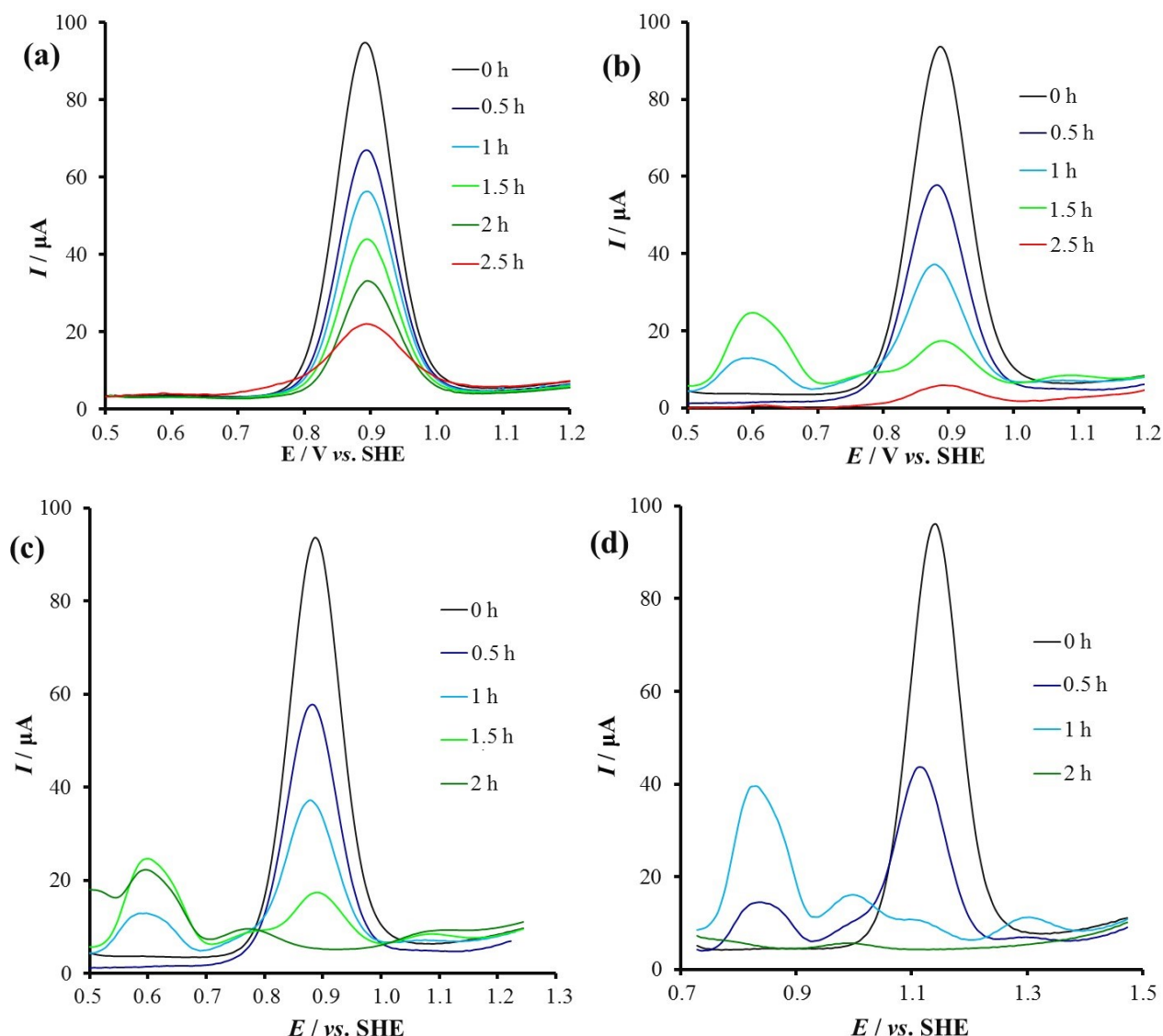


Figure 7. Differential pulse voltammograms of BDD electrode in Britton-Robinson buffer solution containing paracetamol (10 mM) subjected to electrolysis in 0.3 M H₂SO₄ at: (a) 20 mA cm⁻²; (b) 50 mA cm⁻²; (c) 70 mA cm⁻²; (d) 100 mA cm⁻²; T = 25 °C flow rate = 2.7 mL s⁻¹

The effect of the current density on the change of paracetamol concentration during electrolysis was also determined. Figure 8(a) shows the normalized concentration (C/C_0) of paracetamol as a function of the electrolysis time for each of the current density explored. Note that C/C_0 denotes paracetamol concentration at any time to that at the initial time. Exponential decrease of the normalized paracetamol concentration versus the electrolysis time is observed, regardless of the applied current density. The shapes of these curves are in accordance with those described in literature [24] insofar as the applied current densities are higher than the initial limiting current density which is equal to 6 mA cm⁻². In this case, the oxidation process of paracetamol is under mass transfer control. According to our results, the oxidation of paracetamol becomes more rapid as the current density increases from 20 to 100 mA cm⁻². The evolution of the current ratio I/I_m of oxidation peak currents of intermediates during the electrolysis was determined for all applied current densities. Figure 8(b) presents the obtained results, showing that at 20 mA cm⁻² the production of secondary species is very low compared to those obtained under 50, 70 and 100 mA cm⁻². As shown in Figure 8(b), higher is the current density, the greater is the production of these species and quicker is their complete mineralization.

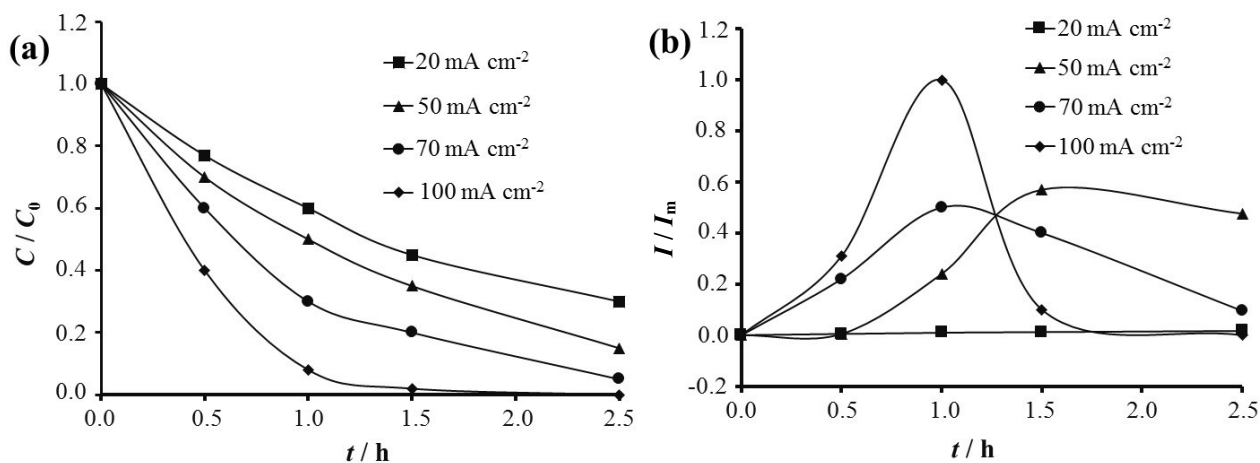


Figure 8. (a) Influence of current density on paracetamol oxidation (10 mM) in 0.3 M sulfuric acid; (b) influence of current density on oxidation of reaction intermediates; $T = 28\text{ }^{\circ}\text{C}$; flow rate = 2.7 mL s^{-1}

Figure 9 highlights the evolution of solution color during the electrolysis. Starting from the colorless solution at the beginning of the experiment, the solution became colored during the experiment, and returned to the colorless solution at the end of the electrolysis. The total discoloration of the solution after 2.5 h of electrolysis may indicate the effectiveness of the treatment at 70 mA cm^{-2} . As mentioned above, before electrolysis, paracetamol solution was colorless and after 0.5 h it becomes colored (yellow color) with an increasing intensity after 1 h of electrolysis. This is followed by a gradual discoloration of the solution, and after 2.5 h, the complete discoloration occurred. Appearance and disappearance of the yellow color during electrolysis could be related to the production of intermediates which undergoes additional oxidation.

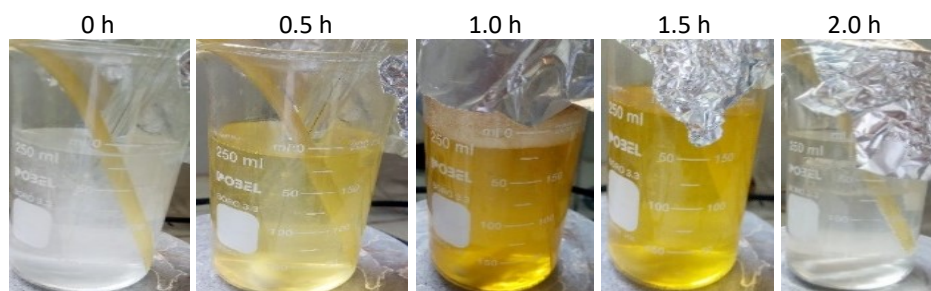


Figure 9. Photos of the evolution of the solution color due to oxidation of intermediates during electrolysis of paracetamol in $0.3\text{ M H}_2\text{SO}_4$ at 70 mA cm^{-2} ; flow rate = 2.7 mL s^{-1}

Current efficiencies of paracetamol oxidation were evaluated as a function of the electrolysis time. The obtained results are presented in Figure 10, showing decrease of oxidation current efficiency with time. The oxidation current efficiencies obtained after 2.5 h of electrolysis at 20, 50, 70 and 100 mA cm^{-2} were 52, 27.5, 22.85 and 19.11 %, respectively. These data show that as the current density increases, a significant part of the current is lost by the production of some side reactions. Low current efficiencies obtained at high current density can be explained by a limitation by mass transport of paracetamol due to parallel formation and oxygen bubbles evolution during electrolysis. The paracetamol oxidation is therefore more and more favorable as the current density decreases.

The influence of paracetamol concentration on the extent of its oxidation during electrolysis was also studied. Figure 11(a) illustrates the results obtained under the current density of 70 mA cm^{-2} at pH 0.6. It is obvious from this figure that the ratio of paracetamol concentration at any time to that at the initial time (C/C_{0t}) decreases with time. After 1 h of electrolysis, the determined oxidation efficiencies for 10, 6 and 1 mM of paracetamol, were found to be 60, 78 and 99 %, respectively.

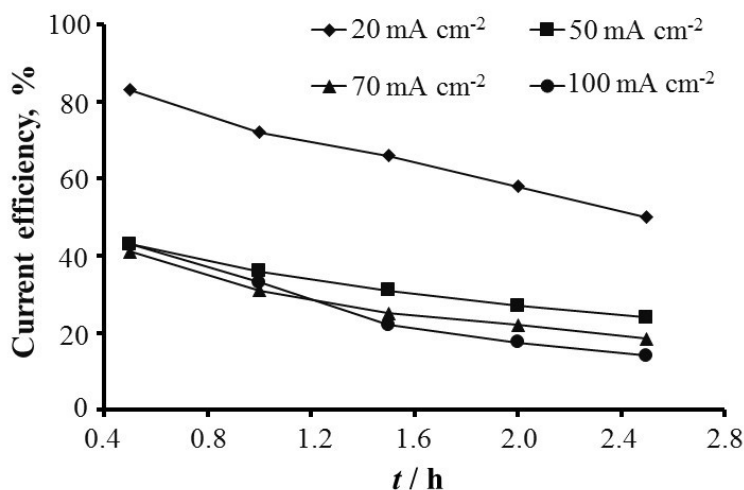


Figure 10. Influence of current density on current efficiency for paracetamol oxidation (10 mM) in 0.3 M H₂SO₄, pH = 0.6; T = 25 °C; flow rate = 2.7 mL s⁻¹

The paracetamol conversion (degradation) rate (τ_0) is followed at any time of the electrolysis by the following equation:

$$\tau_0 = \left(1 - \frac{C}{C_0}\right) 100 \quad (4)$$

The histogram presented in Figure 11(b) shows that oxidation of paracetamol is more favored at low concentrations, suggesting thus more difficult oxidation at increased concentrations of paracetamol. Increase in paracetamol concentration implies increase in the number of collisions between the molecules itself, decreasing at the same time their interaction with hydroxyl radicals (OH·) that are mediators in the oxidation process. The produced quantity of OH· becomes insufficient for total mineralization of paracetamol molecules present on the electrode surface, because of very short lifetime and possible recombination of hydroxyl radicals [21].

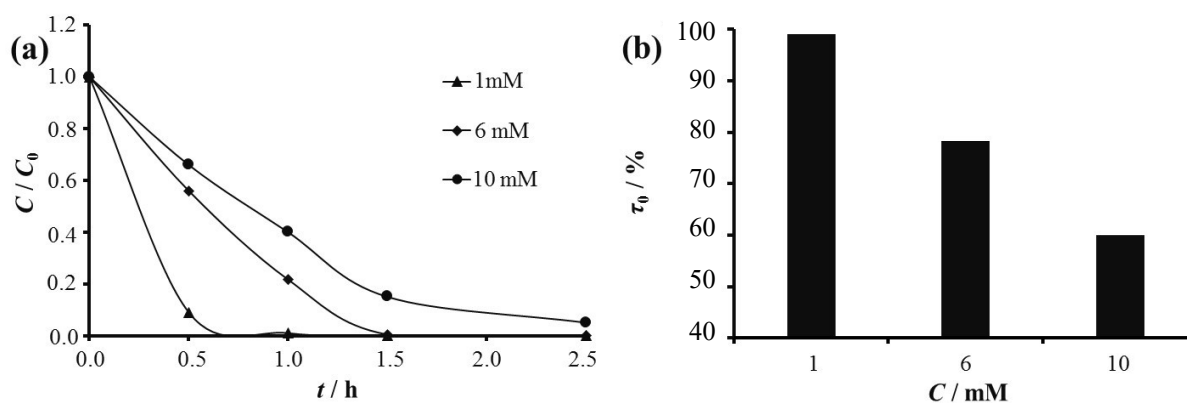


Figure 11. (a) Influence of paracetamol concentration on oxidation by electrolysis in 0.3 M sulfuric acid, pH 0.6, (b) degradation rates for different paracetamol concentrations after 1 h of electrolysis; $j = 70 \text{ mA cm}^{-2}$; T = 28 °C; flow rate = 2.7 mL s⁻¹

The influence of the concentration of paracetamol on the current efficiency of oxidation is also studied and the results are presented in Figure 12. This figure shows that when the concentration of paracetamol decreases, the current efficiency of oxidation increases. Quick reactions take probably place in the reaction medium between paracetamol molecules and oxidative species (OH· in this case), because of high availability of the organic compound. Therefore, the competitiveness of unwanted reactions becomes weak, and several hydroxyl radicals can react with paracetamol molecules.

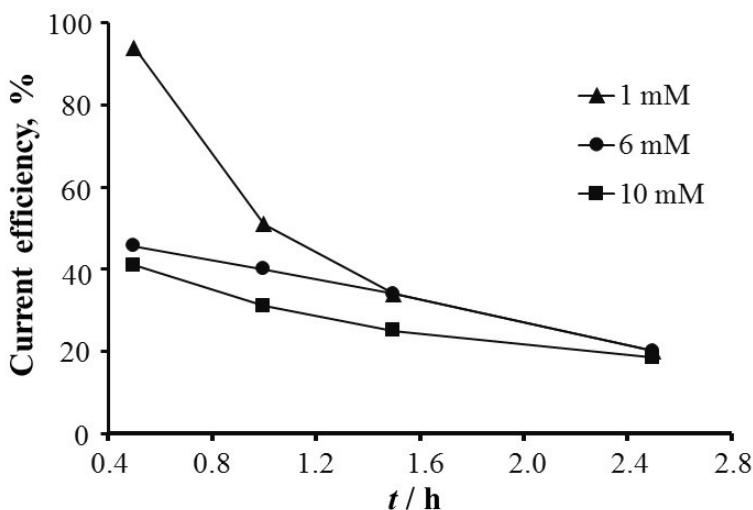


Figure 12. Influence of paracetamol concentration on current efficiency of oxidation at various electrolysis time in 0.3 M sulfuric acid, pH 0.6, $j = 70 \text{ mA cm}^{-2}$; $T = 28 \text{ }^\circ\text{C}$; flow rate = 2.7 mL s^{-1}

Studies focusing on the influence of the initial pH value of the solution were already carried out by large number of environmental scientists in order to weigh its importance in the effectiveness of degradation of pollutants [45,46]. Conflicting results were generally obtained, what is in large part due to the difference in structure of the studied compounds and nature of the electrode material used [47]. Therefore, it becomes necessary to investigate, the effect of the solution initial pH on the electrochemical oxidation of paracetamol on BDD electrode. Figure 13(a) shows the obtained results in the sulfuric acid medium, with initial pH values adjusted to 0.6, 3 and 7 with HCl or NaOH solutions. Figure 13(a) shows that paracetamol oxidation reaction is more rapid at pH 3 than at pH 0.6 and 7. Mineralization rates of paracetamol determined after 1 h of electrolysis at pH 0.6, 3 and 7 were 79, 84 and 74 %, respectively. The high performance of BDD electrode observed in the acidic solutions could be mainly due to the oxidation of paracetamol by the electrogenerated hydroxyl radicals. In the acidic medium, hydrophobicity that results from BDD surface termination changes at high potentials and hampers adsorption of hydroxyl radicals on BDD surface. Thus, hydroxyl radicals are left to react actively with the organic compounds. Besides this indirect oxidation process of paracetamol with $\text{OH}\cdot$, a direct electron transfer reaction between paracetamol and the surface of BDD occurs [48]. Moreover, it is shown in Figure 13(b), that in the course of the electrolysis process of paracetamol, high amounts of intermediates are produced.

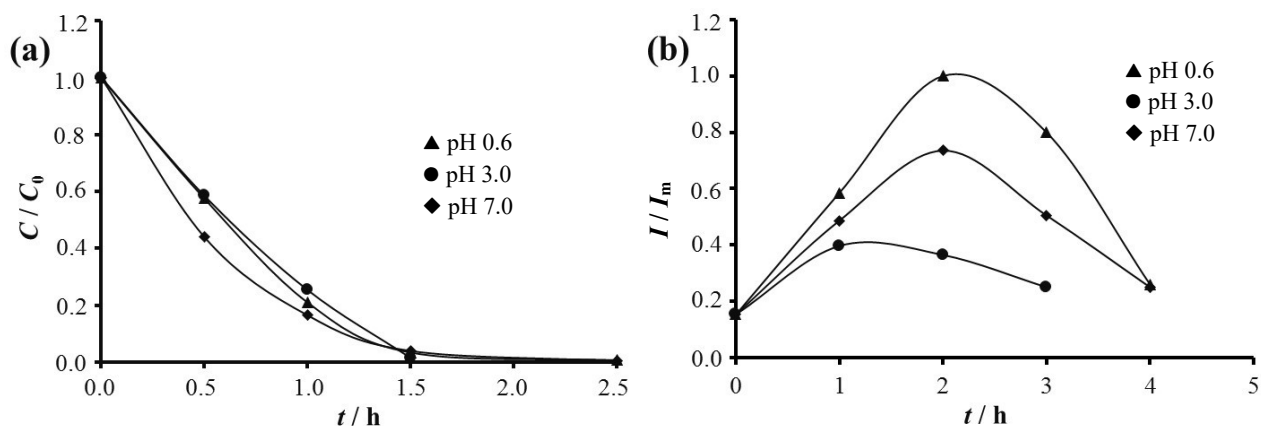


Figure 13. (a) Influence of pH on paracetamol (10 mM) oxidation by electrolysis in 0.3 M sulfuric acid; (b) evolution of the ratio of oxidation peak intensities during electrolysis; $j = 70 \text{ mA cm}^{-2}$; $T = 28 \text{ }^\circ\text{C}$; flow rate = 2.7 mL s^{-1}

Because of the importance of temperature in the physico-chemical analysis and treatment of wastewaters [8,49-51], the effect of temperature on paracetamol oxidation process was also studied in this work. Figure 14(a) presents the obtained results, showing that increase of temperature promotes paracetamol oxidation. Histogram of paracetamol degradation rates determined after 2 h of electrolysis are presented in Figure 14(b). It is obvious that at 28, 55 and 75 °C, 85, 92 and 97 % of paracetamol were degraded, respectively. The exponential decrease of paracetamol concentration during oxidation at all investigated temperatures is characteristic of a pseudo first order reaction.

Figure 15 was built on the basis of Figure 14. From the obtained straight lines in Figure 15(a) that match the pseudo first order reaction model, the kinetic constants of paracetamol oxidation reaction at different temperatures were determined. Thus, at 28, 55 and 75 °C, the determined kinetic constants (k) were 0.9474, 1.1789 and 1.8469 h⁻¹, respectively.

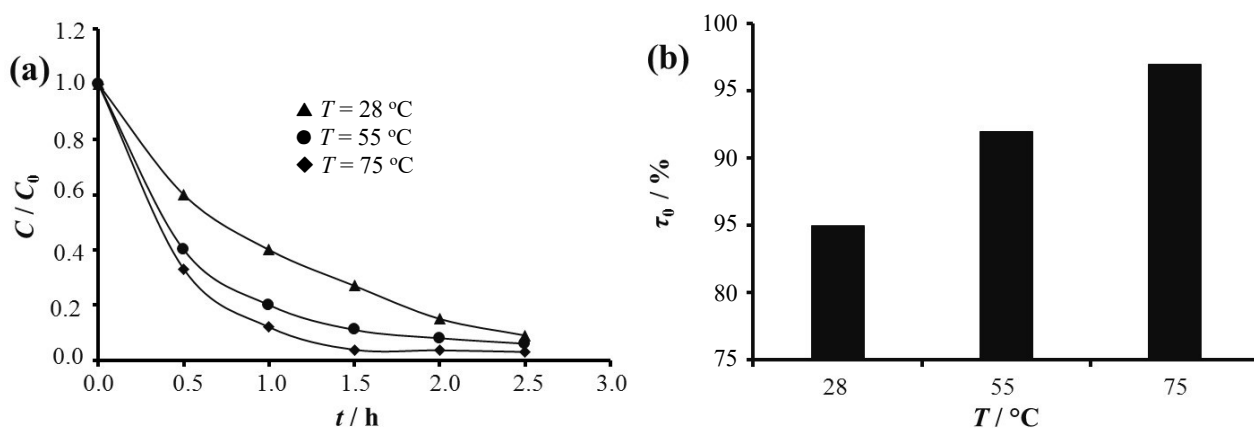


Figure 14. (a) Influence of temperature on paracetamol concentration during electrolysis in 0.3 M H₂SO₄ pH 0.6; (b) degradation rate for different electrolyte temperatures after 2 h of electrolysis at $j = 70 \text{ mA cm}^{-2}$; flow rate = 2.7 mL s^{-1}

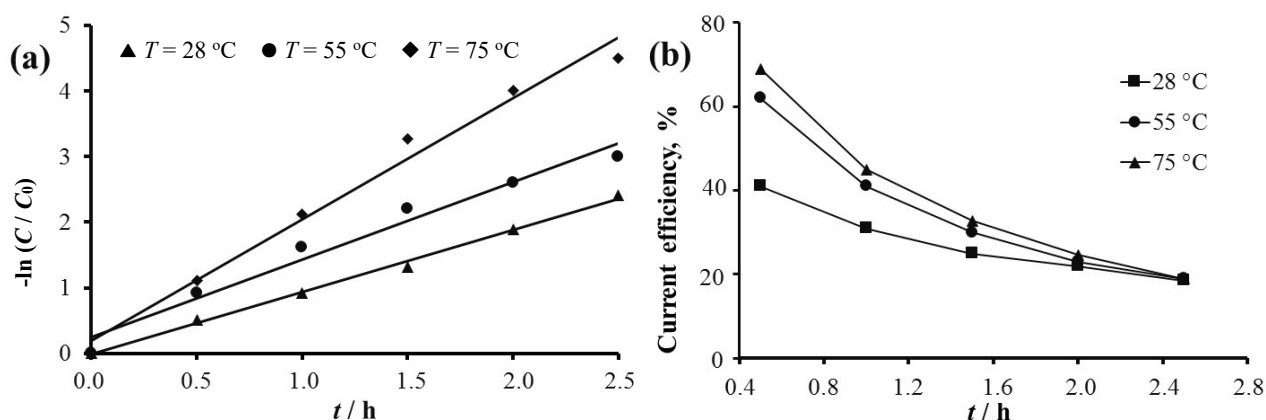


Figure 15. (a) $-\ln(C/C_0)$ as a function of time of paracetamol electrolysis in 0.3 M H₂SO₄ at different temperatures; (b) influence of temperature on current efficiency of paracetamol oxidation at $j = 70 \text{ mA cm}^{-2}$; flow rate = 2.7 mL s^{-1}

These values undoubtedly show that the increase in temperature accelerates and therefore promotes degradation kinetics of paracetamol. It seems that increase in disorder takes place in the reaction medium when the temperature increases, and such effect promotes a higher abatement rate of paracetamol. This situation leads to an increase in shocks between molecules and interactions between species of the medium, accelerating thus paracetamol oxidation by hydroxyl radicals.

The influence of temperature of the supporting electrolyte on the current efficiency of paracetamol oxidation was also investigated. The obtained results are shown in Figure 15(b), suggesting

that the current efficiency increases with the supporting electrolyte temperature. This result shows that increasing the temperature of the support electrolyte helps to reduce the current loss during the electrolysis.

Conclusion

The electrochemical characterization of BDD electrode showed its almost metallic character, indicating that it can be used as the electrochemical sensor for detection and quantification of paracetamol in different solutions. Determination of paracetamol using differential pulse voltammetry was shown to be more reliable in Britton-Robinson buffer solution than in sulfuric and orthophosphoric acids. Oxidation peak of paracetamol was obtained at around 0.9 V vs. SHE, while after the electrolysis in 0.3 M H₂SO₄, another peak related to the oxidation of paracetamol appeared at around 0.55 V vs. SHE. Varying the current density of electrolysis from 20 to 100 mA cm⁻², the total and rapid mineralization of paracetamol was observed at the highest current density and the process was under the mass transport control. By varying the initial concentration of paracetamol during electrolysis, it was shown that paracetamol oxidation kinetic is rapid at low paracetamol concentrations. This study also showed that the oxidation of paracetamol is favored in an acidic medium, particularly at pH 3. Thus, the oxidation efficiency reached 99 % for 1 mM of paracetamol in 0.3 M H₂SO₄, pH 3, after 1 h of electrolysis under the current density of 70 mA cm⁻². It was also found that increase of temperature promotes the degradation rate of paracetamol, reaching 97 % at 75 °C after 2 h of electrolysis at the current density of 70 mA cm⁻².

Acknowledgement: We are thankful to the Swiss National Funds for its financial support. They funded the project (IZ01Z0_146919) which durability helped this work to be undertaken.

References

- [1] M. K. Konan, L. Ouattara, *REVIST-Revue Ivoirienne des Sciences et Technologie* **34** (2019) 44-66 https://revist.net/REVIST_34/REVIST_34_4.pdf.
- [2] T. R. Ferreira, L. C. Lopes, *Jornal de Pediatria (Rio J.)* **92(1)** (2016) 81-87 <http://dx.doi.org/10.1016/j.jpmed.2015.04.007>.
- [3] L. A. Skoglund, E. C. Vigen, P. Coulthard, *British Dental Journal* **228(7)** (2020) 487-487 <http://dx.doi.org/10.1038/s41415-020-1485-y>
- [4] M. Farré, P. N. Roset, S. Abanades, E. Menoyo, Y. Alvarez, M. Rovira, A. M. Baena, *Methods and Findings in Experimental and Clinical Pharmacology* **30(1)** (2008) 37-41 <http://dx.doi.org/10.1358/mf.2008.30.1.1159648>.
- [5] A. Macías-García, J. García-Sanz-Calcedo, J. P. Carrasco-Amador, R. Segura-Cruz, *Sustainability* **11** (2019) 2672 <https://doi.org/10.3390/su11092672>.
- [6] A. G. Al-Kaf, K. M. Najji, Q. Y. M. Abdullah, W. H. A. Edrees, *Chronicles of Pharmaceutical Science* **1(6)** (2017) 341-355.
- [7] L. F. Angeles, R. A. Mullen, I. J. Huang, C. Wilson, W. Khunjar, H. I. Sirotkin, A. E. McElroy, D. S. Aga, *Environmental Science: Water Research & Technology* **6** (2020) 62-77 <https://doi.org/10.1039/C9EW00559E>.
- [8] S. P. Sadia, M. Berté, E. M. H. Loba, F. T. A. Appia, C. Q. -M. Gnamba, I. Sanogo, L. Ouattara, *Journal of Water Resource and Protection* **8** (2016) 1251-1265 <http://dx.doi.org/10.4236/jwarp.2016.813096>.
- [9] H. T. Van, L. H. Nguyen, T. K. Hoang, T. T. Nguyen, T. N. H. Tran, T. B. H. Nguyen, X. H. Vu, M. T. Pham, T. P. Tran, T. T. Pham, H. D. Nguyen, H. -P. Chao, C. -C. Lin, X. C. Nguyen, *Environmental Technology & Innovation* **18** (2020) 100670 <https://doi.org/10.1016/j.eti.2020.100670>.
- [10] F. T. A. Appia, C. Q. -M. Gnamba, O. Kambiré, M. Berté, S. P. Sadia, I. Sanogo, L. Ouattara, *Journal of Electrochemical Science and Technology* **7 (1)** (2016) 82-89 <http://dx.doi.org/10.5229/JECST-.2016.7.1.82>.

- [11] L. A. G. Pohan, O. Kambiré, M. Nasir, L. Ouattara, *Modern Research in Catalysis* **9** (2020) 47-61 <https://doi.org/10.4236/mrc.2020.94004>.
- [12] O. Kambiré, L. A. G. Pohan, S. P. Sadia, K. E. Kouadio, L. Ouattara, *Mediterranean Journal of Chemistry* **10(8)** (2020) 799-808 <http://dx.doi.org/10.13171/mjc10802010271525ko>.
- [13] Y. U. Kouakou, K. F. Essy, A. Dembélé, Y. S. Brou, S. A. Ello, B. I. M. Gouli, A. Trokourey, *Bulletin of the Chemical Society of Ethiopia* **31(3)** (2017) 397-409 <http://dx.doi.org/10.4314/bcse.v31i3.4>.
- [14] U. P. Gnonsoro, K. M. Yao, B. L. Yao, A. M. Kouassi, A. Dembélé, Y. U. Kouakou, K. P. H. Ouattara, D. Diabaté, A. Trokourey, *International Journal of Biological and Chemical Sciences* **9(5)** (2015) 2701-2711 (in France) <http://dx.doi.org/10.4314/ijbcs.v9i5.39>.
- [15] U. Kouakou, A. S. Ello, J. A. Yapó, A. Trokourey, *Journal of Environmental Chemistry and Ecotoxicology* **5(6)** (2013) 168-171 <https://doi.org/10.5897/JECE2013.0264>.
- [16] M. Farhadian, D. Duchez, C. Vachelard, C. Larroche, *Water Research* **42(6-7)** (2008) 1325-1341 <https://doi.org/10.1016/j.watres.2007.10.021>.
- [17] Y. L. Hsiao, K. Nobe, *Journal of Applied Electrochemistry* **23(9)** (1993) 943-946 <https://doi.org/10.1007/BF00251031>.
- [18] C. Comninellis, *Electrochimica Acta* **39** (1994) 1857-1862 [https://doi.org/10.1016/0013-4686\(94\)85175-1](https://doi.org/10.1016/0013-4686(94)85175-1).
- [19] M. H. Zhou, Q. Z. Dai, L. C. Lei, C. A. Ma, D. H. Wang, *Environmental Science and Technology* **39** (2005) 363-370 <https://doi.org/10.1021/es049313a>.
- [20] O. Kambire, F. T. A. Appia, L. Ouattara, *REVIST-Revue Ivoirienne des Sciences et Technologie* **25** (2015) 21-33.
- [21] G. C. Quand-Meme, A. F. T. Auguste, L. E. M. Hélène, B. Mohamed, S. S. Placide, I. Sanogo, L. Ouattara, *Journal of Advanced Electrochemistry* **2(2)** (2016) 85-88.
- [22] M. Berté, F. T. A. Appia, I. Sanogo, L. Ouattara, *International Journal of Electrochemical Science* **11** (2016) 7736-7749 <https://doi.org/10.20964/2016.09.44>.
- [23] A. L. G. Pohan, L. Ouattara, K. H. Kondro, O. Kambiré, A. Trokourey, *European Journal of Scientific Research* **94(1)** (2013) 96-108.
- [24] C. Q.- M. Gnamba, F. T. A. Appia, E. M. H. Loba, I. Sanogo, L. Ouattara, *Journal of Electrochemical Science and Engineering* **5(2)** (2015) 129-143 <https://doi.org/10.5599/jese.186>.
- [25] E. R. Sartori, R.A. Medeiros, R.C. Rocha-Filho, O. Fatibello-Filho, *Journal of Brazilian Chemical Society* **20(2)** (2009) 360-366 <https://doi.org/10.1590/S0103-50532009000200022>.
- [26] G. Tigari, J.G. Manjunatha, *Monatshefte für Chemie - Chemical Monthly* **151** (2020) 1681-1688 <https://doi.org/10.1007/s00706-020-02700-8>.
- [27] P. A. Pushpanjali, J. G. Manjunatha, G. Tigari, S. Fattepur, *Analytical & Bioanalytical Electrochemistry* **12(4)** (2020) 553-568.
- [28] G. Tigari, J. G. Manjunatha, *Journal of Science: Advanced Materials and Devices* **5(1)** (2020) 56-64 <https://doi.org/10.1016/j.jsamd.2019.11.001>.
- [29] J. G. Manjunatha, M. Deraman, N. H. Basri, I. A. Talib, *Arabian Journal of Chemistry* **11(2)** (2018) 149-158 <http://dx.doi.org/10.1016/j.arabjc.2014.10.009>.
- [30] J. E. Reynolds III, M. Josowicz, R. B. Vegh, K. M. Solntsev, *Chemical Communications* **71** (2013) 7755-7862 (Electronic Supplementary Information).
- [31] K. M. Koffi, L. Ouattara, *American Journal of Analytical Chemistry* **10** (2019) 562-578 <https://doi.org/10.4236/ajac.2019.1011039>.
- [32] M. L. Fernández, R. Pintelon, A. Hubin, *Journal of Electroanalytical Chemistry* **720** (2014) 147-155 <https://doi.org/10.1016/j.jelechem.2014.03.024>.
- [33] D. Ersin, H. Silah, *Chemosensors* **8(2)** (2020) 25. <https://doi.org/10.3390/chemosensors8020025>
- [34] F. Bottari, G. Moro, N. Slegers, A. Florea, T. Cowen, S. Piletsky, A.L.N. van Nuijs, K. De Wael, *Electroanalysis* **32** (2020) 135-141 <https://doi.org/10.1002/elan.201900397>.
- [35] M. Q. Li, L. Jing, *Electrochimica Acta* **52** (2007) 3250-3257 <https://doi.org/10.1016/j.electacta.2006.10.001>.
- [36] R. N. Goyal, S. P. Singh, *Electrochimica Acta* **51** (2006) 3008-3012 <https://doi.org/10.1016/j.electacta.2005.08.036>.
- [37] Y. Fan, J. -H. Liu, H. -T. Lu, Q. Zhang, *Colloids and Surfaces B: Biointerfaces* **85** (2011) 289-292 <https://doi.org/10.1016/j.colsurfb.2011.02.041>

- [38] M. P. N. Bui, C. A. Li, K. N. Han, X. H. Pham, G. H. Seong, *Sensors and Actuators B* **174** (2012) 318-324 <https://doi.org/10.1016/j.snb.2012.08.012>.
- [39] S. A. Kumar, C. F. Tang, S. M. Chen, *Talanta* **76** (2008) 997-1005 <https://doi.org/10.1016/j.talanta.2008.04.057>.
- [40] J. Luo, C. H. Fan, X. H. Wang, R. Liu, X. Y. Liu, *Sensors and Actuators B* **188** (2013) 909-916 <https://doi.org/10.1016/j.snb.2013.07.088>.
- [41] S. B. Tanuja, K. Swamy, K. V. Pai, *Journal of Electroanalytical Chemistry* **798** (2017) 17-23 <https://doi.org/10.1016/j.jelechem.2017.05.025>.
- [42] M. X. Zheng, F. Gao, Q. X. Wang, X. L. Cai, S. L. Jiang, L. Z. Huang, F. Gao, *Materials Science and Engineering C* **33** (2013) 1514-1520 <https://doi.org/10.1016/j.msec.2012.12.055>.
- [43] Y. E. Bouabi, A. Farahi, N. Labjar, S. E. I. Hajjaji, M. Bakasse, M. A. E. I. Mhammedi, *Materials Science and Engineering: C* **8** (2016) 70-77 <https://doi.org/10.1016/j.msec.2015.08.014>.
- [44] M. M. Charithra, J. G. Manjunatha, *Journal of Electrochemical Science and Engineering* **10(1)** (2020) 29-40 <http://dx.doi.org/10.5599/jese.717>.
- [45] F. Z. Yehia, G. Eshaq, A. M. Rabie, A. H. Mady, A. E. ElMetwally, *Egyptian Journal of Petroleum* **24** (2015) 13-18 <https://doi.org/10.1016/j.ejpe.2015.03.002>.
- [46] A. M. Muskus, M. Krauss, A. Miltner, U. Hamer, K. M. Nowak, *Environmental Pollution* **259** (2020) 113767 <https://doi.org/10.1016/j.envpol.2019.113767>.
- [47] E. E. Ebrahiem, M. N. Al-Maghrabi, R. M. Ahmed, *Arabian Journal of Chemistry* **10(2)** (2017) S1674-S1679 <https://doi.org/10.1016/j.arabjc.2013.06.012>.
- [48] M. Panizza, G. Cerisola, *Electrochimica Acta* **49(19)** (2004) 3221-3226 <https://doi.org/10.1016/j.electacta.2004.02.036>.
- [49] M. D. G. de Luna, M. L. Veciana, C. -C. Shu, M. -C. Lu, *Journal of Hazardous Materials* **217-218** (2012) 200-207 <https://doi.org/10.1016/j.jhazmat.2012.03.018>.
- [50] I. Delpla, A. -V. Jung, E. Baurès, M. Clement, O. Thomas, *Environment International* **35(8)** (2009) 1225-1233 <https://doi.org/10.1016/j.envint.2009.07.001>.
- [51] A. Hamid, S. U. Bhat, A. Jehangir, *Applied Water Science* **10** (2020) 24 <https://doi.org/10.1007/s13201-019-1043-4>.
- [52] S. M. Bassem, *Biodiversity International Journal* **4(1)** (2020) 10-16 <https://doi.org/10.15406/bij.2020.04.00159>.